

# Lumped parameter model of vane pumps developed in OpenModelica environment.

Barbara Zardin\*<sup>1</sup>, Giovanni Cillo<sup>2</sup>, Marco Rizzoli<sup>2</sup>, Massimo Borghi<sup>1</sup>

<sup>1</sup> Fluid Power Lab, Engineering Department Enzo Ferrari, via P. Vivarelli 10, 41125, Modena, Italy

<sup>2</sup> SmartFluidPower, SpinOff @ University of Modena and Reggio Emilia, via P. Vivarelli 2, 41125, Modena, Italy

**Abstract.** In this paper, the authors present a 0D fluid dynamic model of a vane pump used to refill tanks with fuel. The model is entirely developed in OpenModelica environment, where the authors have created specific libraries of elements suitable for the physical modelling of fluid power components and systems. Among the different approaches, the zero-dimension (0D) fluid-dynamic modelling of positive displacement machines is suitable to study many aspects as: the instantaneous flow rate, pressure and torque transients, the fluid borne noise related to the flow rate and pressure irregularity, the dynamic behaviour of the variable displacement control. Overall, this approach in modelling allows to link the geometrical features of the machine with its dynamic behaviour and for this reason is particularly useful in guiding the design. The model of the vane pump is described together with the main design features that can be analysed in terms of their influence on the pump behaviour. Besides the specific results obtained regarding the design of the pump, the paper also demonstrates the use of OpenModelica language and environment, and its efficacy, into the applications of fluid power modelling and simulation.

## 1 Introduction

Fluid power systems are used in many industrial and mobile applications, thanks to some very valuable characteristics such as the high power to weight ratio, the flexibility and good controllability, the possibility to manage very high loads both with rotary and linear actuators. The main counterpart of these systems is their efficiency, though. For this reason, in last decades, researchers of the field have focused more and more in optimizing the design ([1, 2]), reducing dissipations ([3]), proposing new circuit's layouts ([4, 5]), improve the efficiency and performances of the single components of the systems ([6, 7, 8]). Positive Displacement Machines (PDMs), widely used in fluid power systems for mobile and industrial applications, still present many challenges related to their design. The total efficiency is one of these critical issues: it is determined by volumetric, mechanical and viscous losses that are certainly influenced also by the design choices. The optimum compromise would be to obtain a high and stable value of the total efficiency, in the entire operating range of the machine, but this is a very challenging task. Thus, modelling and simulation have been used in the last decades on the different architectures of PDMs to help designers improving their performance. ([9, 10, 11]). Noise emission is another critical issue regarding PDMs, especially in those applications where the internal combustion engine can be replaced with an electric motor. Accurate design of the machine architecture, especially the low and high pressure ports timing and shape, is essential to improve the flow rate irregularity and the pressure ripple and to take care of this issue. Besides experimental analysis, lumped parameter modelling, FEM modelling and analysis of vibrations may help the designer to prototype new solutions ([12, 13]). Cavitation and aeration affect both the machine efficiency and the noise emissions, as well as the duration of the component. This issue is very challenging to be simulated but advanced CFD analysis combined with lumped parameters approach and experimental vibrational analysis are able to locate the areas where these phenomena occur and to test any design solution introduced to avoid or limit the damage ([14, 15, 16]). No surprises, hence, that modelling and simulation have become essential when addressing the design of PDMs to improve the performances under different aspects. In this paper, an analysis through modelling and simulation for a low pressure vane pump is realized. The manufacturer was particularly interested in analysing different designs of the stator internal surface on the instantaneous pressure transient within the pumping chambers, on the flow rate transient, on the occurring of pressure peaks or local depressurization. The approach followed to create the model is the typical lumped parameters approach, as described for

\* Corresponding author: [barbara.zardin@unimore.it](mailto:barbara.zardin@unimore.it)

similar kind of pumps in ([17-23]). In this work, the method for the geometry definition of the main variables adopted in [17] and [18] was adapted to consider the differences in the stator and vanes design of the pump analysed in this paper, and was implemented in OpenModelica environment [24, 25], using a special set of models created by the authors to study hydraulic components and systems. ([26]).

In the following sections the reader will find: a description of the pump analysed, a description of the mathematical model and of its implementation in OpenModelica and a discussion of the results obtained from the simulations.

## 2 Vane Pump

Vane pumps are PDMs realized coupling an eccentric rotor connected to the pump shaft inside a stator having an internal surface of circular or elliptic or even different profile. The rotor is equipped with several radial or inclined slots where the vanes can slide. The inter-vanes volumes (the volumes confined between two vanes, the rotor and the stator surfaces) are variable volume chambers as function of the shaft angular position and are connected to the low pressure during the phase of increasing volume and with the high pressure port during the decreasing of the volume. In that way, a definite volume of fluid is transferred from the low to the high pressure side at each shaft complete rotation. It is required that the vanes remain in contact with the stator internal surface during the rotation of the rotor, to allow the definition of the separated variable volume chambers. The centrifugal force may be not enough to push the vanes against the stator, so in our design the vanes present channels throughout their length to bring the pressure that is inside the inter-vanes chamber below the vane itself, creating a force that is proportional to the pressure, which pushes the vane outside. The vanes are inclined, as shown in Fig. 1, and the pump has radial ports for the suction and delivery of flow rate. The pump works at low pressure, to deliver fluid in fuel filling systems; since the delivery pressure is low, the pump is not hydraulically balanced with axial elements.

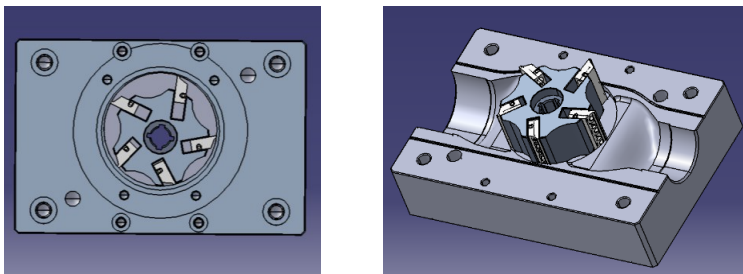
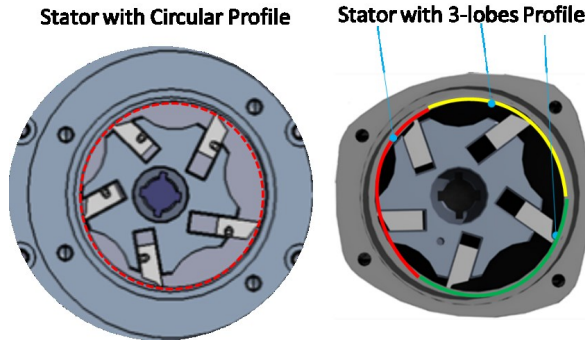


Fig. 1 CAD models of the vane pump analysed

Different stator internal surface profile may be used for this pump: in particular, for the pump studied, a circular profile and a special “3-lobes” profile have been analysed (Fig. 2). With the classical circular profile, there are two critical moments for the pressure transient inside the inter-vanes volume, when the volume is almost isolated from the suction and delivery ports, but is changing due to the rotation of the rotor. While approaching the delivery, after having reached its maximum value, the volume starts decreasing and a pressure peak arises within the chamber; while the volume is approaching the suction, after reaching its minimum value, the volume starts increasing to recall fluid from the low pressure port and a depressurization of the chamber may occur. This pressure transients, characterized by positive and negative peaks and repeated for each inter-vanes volumes, create noise, vibration, affect the flow rate and pressure ripples. During the negative peaks, the pressure can decrease under the saturation pressure of the gas entrained in the fluid, provoking the freeing of gas bubbles (air) and may even reach the vapour pressure of the fluid, causing cavitation. Both aeration and cavitation need to be avoided or limited, since they affect the volumetric efficiency, create noise and damage at the pump components, once the air or vapour bubbles implodes when reaching a higher pressure zone inside the pump. The aim of the alternative “3-lobes” profile is to maintain the volume of the inter-vanes chamber constant during the phases in which the volume is isolated, i. e. not connected with the suction or the delivery port. In that way, the designer would like to avoid or limit the positive and negative pressure peaks. Another way to reduce the peaks is to modify the low and high pressure ports in a way that the inter-vanes volume is never actually isolated. In this way, however, a crossing of the ports is allowed, i. e. for a certain angular interval the volume may be connected with both the ports, thus generating a back flow that negatively affects the volumetric efficiency. In this pump, where there's no hydraulic axial balance for the axial gaps and the leakages are already pretty high, this design solution may not be the best choice.



**Fig. 2** Qualitative comparison of the circular and 3-lobes profile

In order to evaluate how these design modifications can affect the pressure  $p$  transients within the volumes, the flow and pressure ripples, the continuity equation for a control volume  $V$  that exchanges flow rates  $Q_i$  with the low and high pressure ports, should be written and numerically solved. Equation 1 reports the continuity equation written for the control volume  $V$  of fluid with Bulk modulus  $B$ , in the time  $t$  domain and considering an isothermal condition.

$$\frac{dp}{dt} = \frac{B}{V} \left( \sum_i Q_i - \frac{dV}{dt} \right) \quad (1)$$

It is clear now that, to obtain the pressure transient, the flow rates exchanged through the low and high pressure ports and the volume transient have to be expressed as function of the geometrical features of the pump. Besides, considering a constant angular speed for the pump, it is convenient to look at the pressure and volume transients as function of the angular position  $\varphi$  of the pump shaft as shown in equation (2).

$$\omega = \frac{d\varphi}{dt} \rightarrow \frac{dp}{d\varphi} = \frac{B}{\omega \cdot V} \left( \sum_i Q_i - \frac{dV}{d\varphi} \cdot \omega \right) \quad (2)$$

### 3. Description of the main geometrical features and their calculation.

#### 3.1 Stator with circular profile

The methods to define the geometrical features of a vane pump are well described in [17]. Among the different methods explored, it was decided here to write the volume variation as a function of the angular position of the inter vanes chamber, that is rotating with the pump rotor. It is then possible to obtain the volume trend by numerically solving the equation obtained (equation (3)). With respect to what developed in [17], here the expression has been modified first to take into account the different shape of the vane and its inclination  $\alpha$  with respect to the radial direction, still considering the case of a circular internal surface profile for the stator.

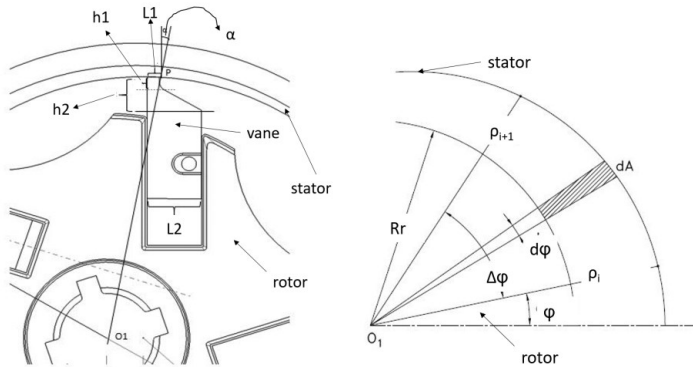


**Fig. 3** Technical drawing of a portion of the vane pump with the quotation of the parameters and variables used in equation (3)

The equation is formulated to evaluate the volume variation  $dV_i$  in correspondence of an angular rotation  $d\phi$ , defining the ray vectors  $\rho_i$  as in Fig. 3 and considering the actual shape and direction of the vanes. The width of the vane/rotor is called  $H$ . The vane lift  $h_i$  is along the length of the vane and it is corrected in equation 3 to consider the inclination  $\alpha$ . The parameter  $\gamma_i$  is used to define a variable circumference arc with the rotational angle. This arc is considered as the length of an area that is added/subtracted to the chamber during rotation. It is defined considering the parameters regarding the vane shown in Fig. 3.

$$\frac{dV_i}{d\phi} = \frac{1}{2} H \cdot \left[ \rho_{i+1}^2 - \rho_i^2 - 2 \cdot \frac{A}{H} - 2 \cdot \frac{B}{H} \right]$$

$$A = H \cdot R_r \cdot \frac{dh_i}{d\phi} \cdot \gamma_i \cdot \cos\alpha, \quad B = H \cdot R_r \cdot \left( \frac{L_2}{R_r} - \gamma_i \right) \cdot \frac{dh_i}{d\phi} \cdot \cos\alpha \quad (3)$$

The parameter  $A$  is related to that portion of the vane that enters/exits the volume chamber during the rotation. Note that for a single chamber  $i$  for example the one represented in

Fig. 4, only the vane  $i$  is considered affecting the volume variation, while the vane  $i+1$  will affect the following chamber  $i+1$ . This is an approximation, but was considered acceptable given the position of the contact points  $P_i$  and  $P_{i+1}$  of the vanes at the stator surface.

The parameter  $B$  is defined to consider that portion of volume that is isolated when the vane is completely inside its slot and joins the chamber volume when the vane is going out from the slot.

At this point to calculate the volume transient as a function of the angular position  $\phi$  a code in OpenModelica was written and the backward finite difference method was applied to numerically find the solution.

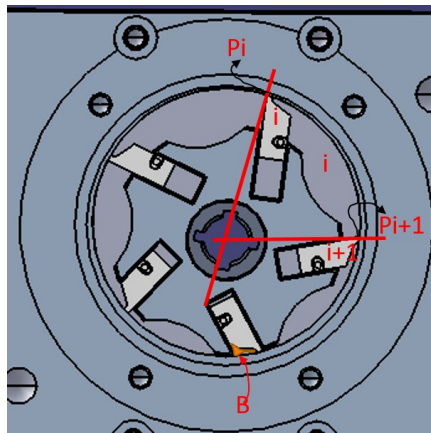


**Fig. 4** View of the internal components of the pump and generic inter-vanes volume chamber

### 3.2 Stator with “3-lobes” profile

An example of what is the “3-lobes” profile for the stator surface is shown in shown in Fig. 5a. With respect to the rotor centre, the profile is made of circumference arcs, each one with its extension with respect to the rotor centre and tangent at the extremities to the neighbouring arcs. Each arc has its own curvature centre and radius, as visible in Fig. 5b, and eccentricity. To adapt the code written for the stator circular profile, the “3-lobes” profile was divided in 9 sectors, defining the different parameters for each of them (radius, eccentricity, angular extension) and applying the same method to calculate the volume transient. Moreover, for each sector, a routine was implemented, to check where the confining vanes of the generic chamber are at a specific angular position (in the sector analysed, in the previous one or in the following one).

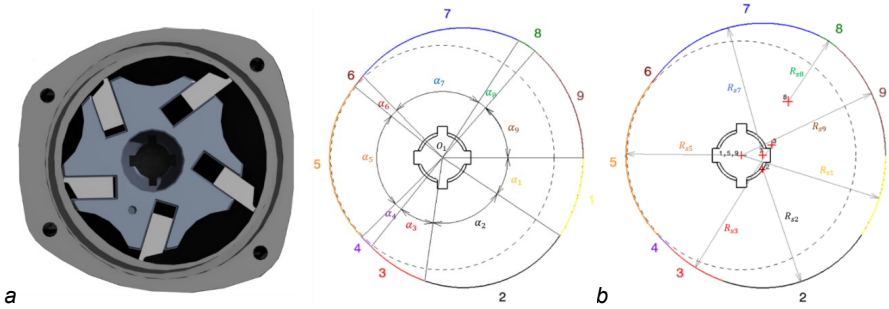


**Fig. 5** View of the design of the pump with the “3-lobes” profile and of the 9 sectors defined for the sake of an easier definition of the profile into the numerical code.

**3.3 High and low pressure ports**

The inter-vanes volume chamber is connected to the low and high pressure radial ports during the suction and delivery phase respectively (Fig. 6). In order to determine the flow rates exchanged by the volume chamber with the ports, it is necessary to determine the flow areas. The flow areas have been determined considering an observer inside the volume chamber, looking at the opening and closing of these passages; during the rotation, the flow area will open as soon as the first vane confining the volume overcomes the opening point of the specific port, then reaches the maximum value when the second vane also overcomes the opening point and successively starts decreasing when the first vane is overcoming the closing point till the total closure when the second vane also overcomes the closing point. The geometry of the ports is quite simple, but the position of the opening and closing points may be critical in determining the angular interval where the volume may be isolated. Moreover, there exist a design of the ports with constant height and a design with variable height. A routine in OpenModelica language has been written to obtain the suction and delivery flow areas for the reference volume chamber.

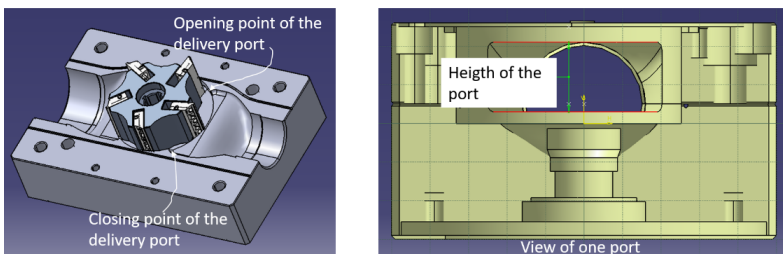


**Fig. 6** The pump and its radial low and high pressure ports.

### 3.4 Geometrical results

In this section the geometrical description of the volume, volume derivative and suction and delivery flow areas are shown for the reference chamber. The other chambers in the pump have the same geometrical features but they are shifted with respect of the reference rotational angle of the quantity  $2\pi/z$ , where  $z$  is the number of vanes ( $z=5$  for the pump analysed). In Fig. 7 the volume and volume derivative of the reference chamber for the circular stator profile are shown, non-dimensioned with respect their maximum values. The trend of the volume with respect to the angular reference position of the volume chamber, which follows the shaft angular position of the pump, is the typical sinusoidal shape that we find in the positive displacement pump for a single pumping chamber: between  $0^\circ$  and  $180^\circ$ , the volume is decreasing and it is connected to the delivery, between  $180^\circ$  and  $360^\circ$ , the volume is increasing and it's connected with the suction port. The orange line in figure is the volume derivative, which is a consequence of the volume trend.

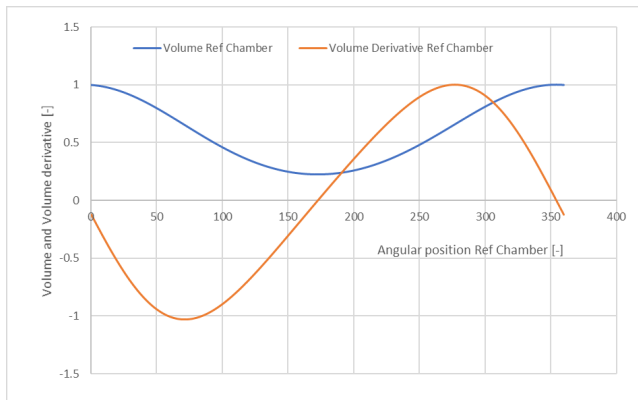


Fig. 7 Volume and volume derivative transient for a reference chamber with respect to the angular position.

In Fig. 8 the volume and volume derivative of the reference chamber for the “3-lobes” stator profile are shown, again non-dimensioned with respect their maximum values.

Moreover, the values obtained from the numerical procedure were compared with the volume evaluation on the CAD model of the pump. The relative error between the two evaluation is smaller than 5% and was considered acceptable for this first version of the model.

The volume trend in this case (blue line) shows a flat profile nearby and around the dead points ( $0^\circ$  and  $180^\circ$ ), thus the volume derivative is almost zero and this helps to avoid aggressive pressure peaks within the chamber, while preserving the volume variation in the rest of the angular interval, which allows delivery of flow and suction from the tank.

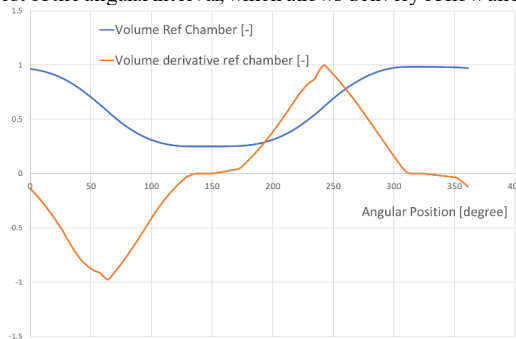
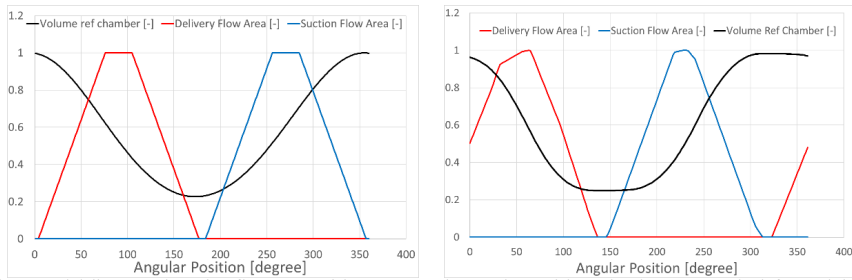


Fig. 8 Volume and volume derivative of the reference chamber for the “3-lobes” stator profile with respect to the angular position.

In Fig. 9 the delivery and suction flow areas together with the volume chamber transient, are shown again with respect to the angular position of the reference chamber, for the two design versions, at left with circular stator profile, at right for the “3-lobes” stator.



**Fig. 9** Volume and delivery and suction flow areas with respect to the angular position, circular stator at the left, “4-lobes” stator at the right.

#### 4. Structure of the model and equations

The lumped parameters fluid - dynamic model of the vane pump is realized by connecting  $z$  variable control volumes ( $z=5$ ). The control volumes are connected to each other with orifices that represent in the model the gaps between the vane tip and the stator surface, the axial gaps between the pump body and the assembly rotor-vanes. Further axial gaps are connecting the control volumes and the drainage.

Two variable orifices, then, represent the connection with the low and high pressure ports. Given its structure, it is easy to modify the model to adapt to the number of vanes by replicating the same basic core unit represented in Fig. 10.

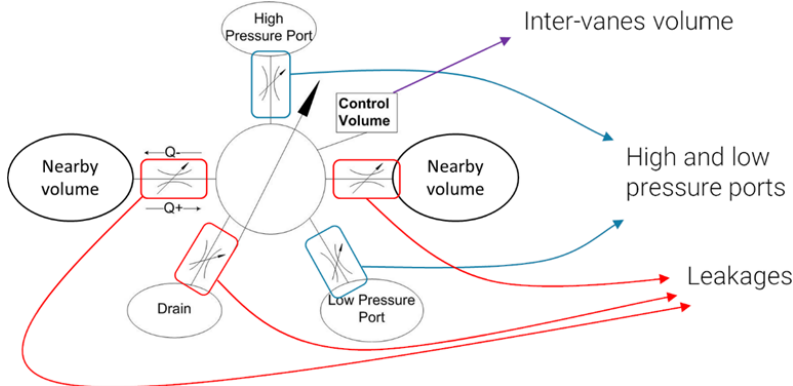


**Fig. 10** Representation of the model of one inter-vanes volume chamber

The model has been implemented in OpenModelica Environment [25], using a set of components created by the authors to specially model fluid power components and systems [26], as shown in Fig. 11.

It's worth noting that here the vanes are represented by moving elements (sliding into their radial slots) connected thorough channels with a volume of fluid at the bottom and with the inter-vanes chamber at the top.

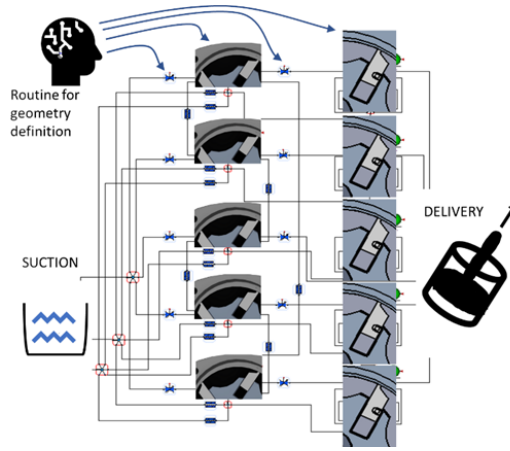


**Fig. 11** A graphical representation of the pump model in OpenModelica environment

The mathematical model, manipulated by the OpenModelica solver, is briefly described in the following. For each control volume, the continuity equation for a control volume is written as in equation (1).

The flow rates exchanged by the control volume with the low and high pressure ports, are expressed using the turbulent orifice equation:

$$Q_{port} = c_d \cdot A(\varphi) \cdot \sqrt{\frac{2|\Delta p|}{\rho}} \cdot \text{sgn}(\Delta p) \quad (4)$$

In this equation,  $C_d$  represents the discharge coefficient, which is defined as a function of the fluid Reynolds number in a way to represent a linear trend at low Reynolds number and a constant value at high Reynolds number;  $A$  is the flow area,  $\Delta p$  is the pressure difference between the port and inter-vanes volume.

The leakages through the gaps listed previously, are expressed using the Hagen-Poiseuille equation and considering the Couette term due to the moving elements. The gaps geometry has been schematized as equivalent rectangular gaps, shaped between a wall that is moving with velocity  $v$  and a wall that is still. The length  $l$ , height  $h$  and width  $b$  of each gap are considered constant in this model. The height  $h$  of the gaps has been set considering the coupling tolerances of the components of the pump. Finally,  $\mu$  is the dynamic viscosity of the fluid.

$$Q_{gap} = \frac{b \cdot h^3}{12 \cdot \mu \cdot l} \cdot \Delta p + \frac{v}{2} \cdot h \cdot b \quad (5)$$

All the geometrical features are determined with the dedicated routine developed in the same environment and completely parametrized in a way to be applicable to different pump designs without complication of the model.

## Pressure and flow rate results

A comparison with available experimental data was performed for a qualitative comparison with the model: in order to compare the simulated results with the real ones, the operating conditions tested at the test rig for the pump equipped with the circular profile were also simulated with the model.

- Inlet pressure = 0.94 bar
- Outlet pressure range = 1.2-2.5 bar
- Pump rotational speed range = 3000 – 3200 – 3400 – 3600 rpm

In Fig. 12 the results obtained at 3000 rpm are shown, as an example. At higher rotational speed, the difference between the numerical and measured flow rate values is similar. There is a maximum relative error of about 5% for the higher delivery pressure values, in any case the difference increases with the delivery pressure value. We have taken this as a sign that a more accurate analysis on the leakages and gaps representation in the model should be introduced in the future. On the other hand, for qualitative comparison between different pump designs the use of the model has been considered appropriate and useful.



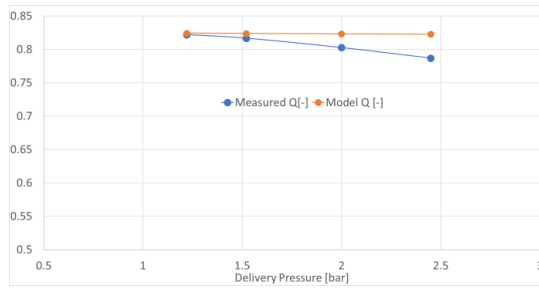


**Fig. 12** Measured and calculated flow rate values at the delivery of the pump with the circular profile stator

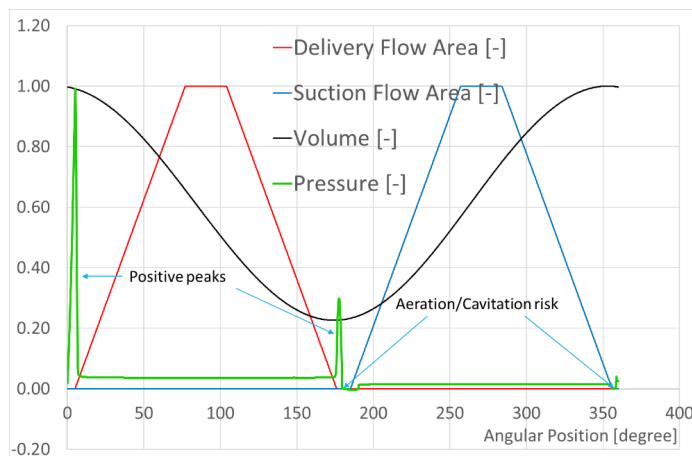


**Fig. 13** Results at 3000 rpm for the pump equipped with the stator with the circular internal surface 's' profile

In Fig. 13 some numerical results are shown for the pump equipped with the circular profile stator. In particular, the pressure transient within the reference inter-vanes chamber is depicted with reference to the angular position of the chamber, together with the suction and delivery flow areas and volume variation in the same angular interval. All the geometrical values are referred to their maximum values. The pressure is referred to the delivery pressure, pm. With this kind of suction and delivery flow areas, there are small angular intervals in which the volume is isolated, with the exception of the leakages. For that reason, pressure peaks arise at the beginning and end of the delivery phase and negative peaks also are visible at the beginning and end of the suction phase. In order to decrease these peaks, design modifications have to be introduced at the ports flow areas or the shape of the stator internal profile, in a way to control the volume trend especially at these critical points. Testing the “3-lobes” stator profile for the pump for the same rotational speed and very similar delivery pressure, leads instead to the results shown in Fig. 14. This time also the volume derivative is shown, to better understand the pressure transient. The fact that the volume almost remains constant with this stator profile in the angular interval where the ports are closing and opening, lead to the disappearing of the positive peaks. A negative peak still is present at the end of suction, when the isolated volume, calculated with the numerical routine is slightly decreasing, but it is soon recovered at the opening of the delivery and it appears to be not dangerous from the aeration/cavitation point of view. To understand better how much of this negative peak is due to the actual volume and volume derivative trends, the accuracy in the determination of the volume derivative through the numerical procedure will be assessed in the future.

In any case, the model is also ready to receive the geometrical data from external analysis/evaluation, to be able to give more accurate results about the pressure transient.

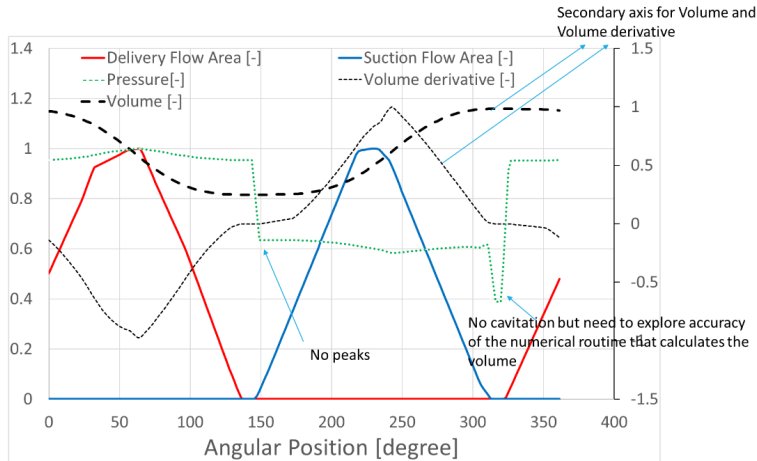


Fig. 14 Results at 3000 rpm for the pump with stator with the “3-lobes” internal surface’s profile

## Conclusion and perspectives

In this paper, a lumped parameters model of a vane pump is realized in OpenModelica environment, using a set of components specifically realized to model fluid power components and systems. The model has been created in a “parametric fashion”. This means that the model can easily be adapted to analyse different design modifications, for example the number of vanes, the suction and delivery flow areas, the stator internal profile.

Well before the realization of a physical prototype, the model is useful to give indications on the impact of the design on the pressure transients inside the volume chambers, pressure and flow ripples, flow rate at the delivery of the pump.

Future developments will be addressed to better describe the gaps inside the pump; this may represent a critical point when we want to be accurate in the pressure negative and positive peaks evaluation. For analogous reason, the routine that determines the geometrical features with special stator profile will be tested with different solution and when possible the results coming from the model will be validated with measurements on the pump prototype.

## Acknowledgements

Authors would like to thank Ing. Enrico Bagni and Ing. Ludovico Posa for the help in developing the OpenModelica code and their work during the master degree’s thesis in Mechanical Engineering at the Fluid Power Lab in Modena.

Moreover, authors would like to thank Piusi SpA, in particular Ing. Fabio Cavaletti and Ing. Giacomo Mazzoni for the support during the design analysis and discussion about the model and results.

## References

1. Rossetti A., Macor A., Scamperle M., Optimization of components and layouts of hydromechanical transmissions, *International Journal of Fluid Power*, Vol. **18**, Issue **2**, Pages 123-134. (2017) DOI: 10.1080/14399776.2017.1296746.
2. Rossetti A., Macor A., Benato A., Impact of control strategies on the emissions in a city bus equipped with power-split transmission, *Transportation Research Part D: Transport and Environment*, Vol. **50**, Pages 357-371. (2017) DOI: 10.1016/j.trd.2016.11.025.
3. Casoli, P., Pompini, N., Riccò, L., Simulation of an Excavator Hydraulic System Using Nonlinear Mathematical Models, *Strojniški vestnik - Journal of Mechanical Engineering* **61**, **10**, 583-593 . (2015) DOI:10.5545/sv-jme.2015.2570

4. Gaiola, A., Zardin, B., Casoli, P., Borghi, M., Mazzali, F., Pintore, F., Fiorati, S., The Hydraulic Power Generation and Transmission on Agricultural Tractors: feasible architectures to reduce dissipation and fuel consumption – Part I, *E3S Web Conf.* **197** 07009 (2020), DOI: 10.1051/e3sconf/2020197070.
5. Casoli, P., Zardin, B., Ardizio, S., Borghi, M., Pintore, F., Mesturini, D., The Hydraulic Power Generation and Transmission on Agricultural Tractors: feasible architectures to reduce dissipation and fuel consumption – Part 2, *E3S Web Conf.* **197** 07010 (2020)
6. Zardin, B., Borghi, M., Cillo, G., Rinaldini, C.,A., Mattarelli, E., Design Of Two-Stage On/Off Cartridge Valves For Mobile Applications, *Energy Procedia*, Volume **126**, 2017, Pages 1123-1130, (2017) . ISSN 1876-6102.
7. Zardin, B., Cillo, G., Borghi, M., D’Adamo, A., Fontanesi, S., Pressure Losses in Multiple-Elbow Paths and in V-Bends of Hydraulic Manifolds. *Energies* 2017, **10**, 788. (2017).
8. Senatore, A., Buono, D., Frosina, E., Pavanetto, M., Costin, I., Olivetti, M., Improving the performance of a two way control valve using a 3D CFD modeling, Proceedings of the ASME *International Mechanical Engineering Congress and Exposition*, (IMECE), 7, Montreal, Canada, DOI 10.1115/IMECE2014-3820, (2014).
9. Zardin, B., Natali, E., Borghi, M., Evaluation of the Hydro—Mechanical Efficiency of External Gear Pumps. *Energies* 2019, **12**, 2468. <https://doi.org/10.3390/en12132468>. (2019).
10. Thiagarajan, D., Vacca, A., Investigation of Hydro-Mechanical Losses in External Gear Machines: Simulation and Experimental Validation. In *Proceedings of the BATH/ASME 2016 Symposium on Fluid Power and Motion Control*, Bath, UK, 7–9 September 2016; p. V001T01A015. (2016).
11. Michael, P., Khalid, H., Wanke, T., An Investigation of External Gear Pump Efficiency and Stribeck Values, *SAE Technical Paper*: No. 2012-01-2041; SAE International: Chicago, IL, USA, (2012).
12. Casoli, P., Pastori, M., Scolari, F., Rundo, M., Active pressure ripple control in axial piston pumps through high-frequency swash plate oscillations – A theoretical analysis, *Energies*, **12** (7), art. no. 1377, DOI: 10.3390/en12071377. (2019).
13. Marinaro, G., Frosina, E., Senatore, A., A Numerical Analysis of an Innovative Flow Ripple Reduction Method for External Gear Pumps, *Energies* 2021, **14**(2), 471, (2021).
14. Siano, D., Frosina, E., Senatore, A., Diagnostic Process by Using Vibrational Sensors for Monitoring Cavitation Phenomena in a Getoror Pump Used for Automotive Applications, *Energy Procedia*, **126**, 1 September 2017, Pages 1115-112. (2017).
15. Casoli, P., Pastori, M., Scolari, F., Rundo, M., A vibration signal-based method for fault identification and classification in hydraulic axial piston pumps, *Energies*, **12** (5), art. no. 953, DOI: 10.3390/en12050953. (2019).
16. Shah, Y.G., Vacca, A., Dabiri, S., Frosina, E., A fast lumped parameter approach for the prediction of both aeration and cavitation in Gerotor pumps, *Meccanica*, **53**(1-2), Pages 175-191, (2018).
17. Mancò, S., Nervegna, N., Rundo, M., and Armenio, G., Modelling and Simulation of Variable Displacement Vane Pumps for IC Engine Lubrication, *SAE Technical Paper* 2004-01-1601, <https://doi.org/10.4271/2004-01-1601>. (2005).
18. Rundo, M., Pavanetto, M., A., Comprehensive Simulation Model of a High Pressure Variable Displacement Vane Pump for Industrial Applications., Proceedings of the ASME International Design Engineering Technical Conferences and Computers and Information in Engineering Conference. Volume **1A**. Quebec, Canada. V01AT02A002. ASME. <https://doi.org/10.1115/DETC2018-85099>. (2018).
19. Rundo, M., Altare, G., Lumped Parameter and Three-Dimensional Computational Fluid Dynamics Simulation of a Variable Displacement Vane Pump for Engine Lubrication., *ASME. J. Fluids Eng.*; **140**(6): 061101. <https://doi.org/10.1115/1.4038761>. (2018).
20. Cantore, G., Milani, M., Paltrinieri, F., Tosetti F., Lumped Parameters Numerical Simulation of a Variable Displacement Vane Pump for High Speed ICE Lubrication, *SAE Technical Paper* 2008-01-2445, (2008).
21. F. Fomarelli, A. Lippolis, P. Oresta, A. Posa, Investigation of a pressure compensated vane pump, *Energy Procedia*, Volume **148**, Pages 194-201, ISSN 1876-6102, <https://doi.org/10.1016/j.egypro.2018.08.068>. (2018).
22. Rundo, M., and Nervegna, N., Geometry Assessment of Variable Displacement Vane Pumps., *ASME. J. Dyn. Sys., Meas., Control.*; **129**(4): 446–455. (2007)
23. Rundo M., Piloted Displacement Controls for ICE Lubricating Vane Pumps, *SAE Int. J. Fuels Lubr.* **2**(2):176-184, <https://doi.org/10.4271/2009-01-2758>. (2010).
24. Tiller, M., Introduction to Physical Modeling with Modelica, *The Springer International Series in Engineering and Computer Science book series* (SECS), Volume **615**, ISBN : 978-1-4613-5615-8. (2001).
25. <https://www.openmodelica.org/>, last access June 24th, 2021.
26. <https://smart.fluidpower.it/>, last access June 24th, 2021.